Development of a High-Resolution Melting (HRM) Assay for DNA Methylation Analysis of the SHANK3 Gene

Sema Tiryaki

Abstract

Background: DNA methylation within CpG islands is a key epigenetic mechanism regulating gene expression. SHANK3 encodes a synaptic scaffolding protein with critical roles in neurodevelopment and synaptic function, and aberrant SHANK3 methylation has been implicated in neuropsychiatric disorders. Reliable locus-specific assays are required to investigate its epigenetic regulation.

Methods: The SHANK3 sequence (NCBI Gene ID: 85358) was screened in silico to identify CpG islands. A CpG-rich region upstream of exon 3 was selected for assay development. Bisulfite-converted sequences representing fully methylated and unmethylated states were aligned, and three primer sets were designed accordingly. Bisulfite conversion was performed using the EZ DNA Methylation™ Kit, and conversion efficiency was confirmed with the DAPK1 control assay and commercially available methylated and unmethylated genomic DNAs. High-resolution melting (HRM) analyses were carried out on LightCycler® 480 and CFX96 platforms.

Results: Primer Sets 1 and 3 consistently amplified the target region and produced distinct melting profiles that discriminated methylated from unmethylated templates, whereas Primer Set 2 was less efficient. Gradient PCR optimization identified 54 °C as the optimal annealing temperature. Non-template controls showed late-cycle amplification and nonspecific products, but these were distinguished by melting temperatures lower than those of the expected amplicon and did not interfere with interpretation.

Conclusion: A locus-specific HRM assay for SHANK3 methylation analysis was successfully developed and optimized. The method enables qualitative discrimination of methylated and unmethylated templates, and provides a robust framework for future validation studies and potential application to clinical investigations of SHANK3 epigenetic regulation.

Introduction

DNA methylation is one of the most studied epigenetic modifications and plays a critical role in gene regulation, chromatin remodeling, and cellular differentiation. Aberrant methylation, particularly in promoter regions, has been consistently associated with transcriptional silencing of tumor suppressor genes and the activation of oncogenic pathways (Druml & Cichna-Markl, 2014; Wu et al., 2017). Promoter hypermethylation is one of the earliest events in carcinogenesis, providing unique opportunities for its use as a biomarker in both diagnostic and prognostic contexts (Zhao et al., 2022; Shi et al., 2019; Zhang et al., 2015). Due to its chemical stability, cancer-type specificity, and translational potential, promoter methylation has emerged as one of the most powerful biomarker candidates in precision medicine (Mio & Damante, 2022; Ma, Cao & Guo, 2016; Dong et al., 2021).

Although most studies have traditionally focused on promoter regions upstream of the first exon, methylation analysis is not restricted to these loci. Several studies have reported methylation in the first exon, internal exons, and intragenic CpG islands, highlighting that exonic methylation may influence transcription regulation, alternative splicing, and gene silencing (Nguyen et al., 2001; Yan et al., 2003; Tang et al., 2012; Laurent et al., 2010; Luo et al., 2018). Thus, the investigation of methylation across exonic regions represents a growing area of research with potential diagnostic relevance.

One gene of particular interest in this context is SHANK3, a postsynaptic density protein-coding gene essential for synaptic organization and function. SHANK3 mutations and epigenetic alterations have been extensively

studied in autism spectrum disorders (ASD), neurodevelopmental disorders (NDDs), and synaptopathies such as Phelan-McDermid syndrome (PMS) (Megagiannis et al., 2022; Cooke et al., 2022; Loth et al., 2017). Gene body methylation of SHANK3 has been linked to downregulation of mRNA expression in animal models (Barua et al., 2014), while promoter methylation has been associated with neurodevelopmental pathways and tissue-specific differentially methylated regions (TS-DMRs) (Grayson & Dunn, 2021). Furthermore, SHANK3 promoter methylation has been proposed as a biomarker in a subset of studies, including peripheral blood-based approaches for schizophrenia (Barua et al., 2014).

Despite the relatively small body of evidence, SHANK3-related genetic and epigenetic changes—including mutations, gene body methylation, and promoter methylation—are increasingly recognized for their diagnostic and therapeutic potential. The exploration of SHANK3 methylation across both promoter and exonic regions may provide novel opportunities for biomarker discovery and for understanding disease mechanisms in ASD, PMS, and schizophrenia.

In this study, rather than limiting our analysis to the commonly investigated promoter region upstream of exon 1, we focused on an exonic CpG island located between exons 2 and 3 of the SHANK3 gene. Our assays were designed to specifically target this region, thereby broadening the scope of SHANK3 methylation analysis beyond the first exon.

Material and Method

1- Selection of Target Region by in silico CpG Island Screening and Primer Design

The SHANK3 gene sequence (NCBI Gene ID: 85358) was examined to identify CpG islands suitable for promoter methylation analysis by HRM. CpG Island Grapher (Hahn Lab utilities, http://canna.cau.ac.kr/util/) was used, with CpG islands defined as regions with GC content >55–60 and a CpG observed/expected (O/E) ratio >0.6. A CpG island fulfilling these thresholds (Figure 1) was identified upstream of exon 3, and a 1,135 bp fragment spanning this region was selected for assay design.

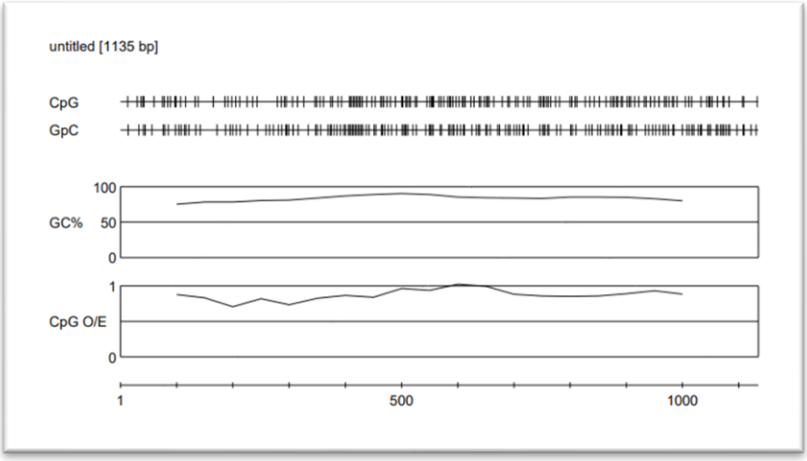

Figure 1. 1000kb upstream Exon 3 CpG island screeening

The “Bisulfite Conversion” tool (Hahn Lab utilities) used to obtain bisulfite-converted (BC) sequences for fully methylated (M) and fully unmethylated (UnM) DNA. The original, M-BC and UnM-BC sequences were aligned (Supplementary Figure S1)

Primers were designed to target regions that remain unchanged after bisulfite conversion, with the following considerations: minimization of cytosines (if unavoidable, only one C and not positioned at the 3′ end), amplicon

size between 80–300 bp, and avoidance of homopolymers, repeats, and 3′ complementarity. Three primer pairs (Primer Sets 1–3) were generated. Candidate primers were evaluated using IDT OligoAnalyzer to assess secondary structures and hairpin formation, and to calculate melting temperatures (Tm). Predicted melting temperatures of the expected amplicons were further determined using Amplicon3Plus (https://www.primer3plus.com/amplicon3plus.html). Oligonucleotides were synthesized commercially (Oligomer Biyoteknoloji, Ankara, Türkiye). The sequences of the primers, their corresponding amplicons, and melting temperatures are summarized in Table 1, 2 and 3.

Table 1. Primer Set 1 primer sequences, amplicon lengths, and melting temperatures for methylated (M) and unmethylated (UnM) templates

Primer Set 1							
SHANK3-F1 primer	TTAATTTCGTTATAGTTTTTTAGATT			SHANK3-R1 primer	AACCAATACTAAAAAATTACTTAC		
LENGTH	26			LENGTH	24		
MELT TEMP	55,8			MELT TEMP	54,8		
Annealing Temp:	52,8			Annealing Temp:	51,8		
Amplicon 1-M				**Amplicon 1-UnM**			
TTAATTTCGTTATAGTTTTTTAGATTTTCGTTTCGTGGTTCGGTTTTCGTTTTTCGTATATATTTTTCGTTTTTATTCGGGATTTCG**TAAGTAATTTTTTAGTATTGGTT**				**ATTTTGTTATAGTTTTTTAGATT**TTTGTTTTGTGGTTTGGTTTTTGTTTTTTGTATATATTTTTTGTTTTTATTTGGGATTTT**GTAAGTAATTTTTTAGTATTGGTT**			
Melt Temp (°C)	78,4	Amplikon Length	106 bp	Melt Temp(°C)	74,7	Amplikon Length	106 bp

Table 2. Primer Set 2 primer sequences, amplicon lengths, and melting temperatures for methylated (M) and unmethylated (UnM) templates

Primer Set 2							
SHANK3-F2 primer	GGTCGATGTAGTTGAGT			SHANK3-R2 primer	TCTACTACAAATCCGAAATAC		
LENGTH	17			LENGTH	21		
MELT TEMP	55,2			MELT TEMP	55,3		
Annealing Temp:	52,2			Annealing Temp:	52,3		
Amplicon 2-M				**Amplicon 2-UnM**			
GGTCGATGTAGTTGAGTCGCGTCGTCGTCGTCGTCGTCGTTTTTGCGGAGTTTTCGGAGTCGTTGTTTTTCGCGTCGGTTTCGGTTTCGGTTTTTTCGGTTTTTTTTCGCGTAGCGCGGTCGACGGGGTTTCGGCGGGGGGGAAGGGGGGGTCGGGCGTCGCGCGGAGTTTTCGGGCGTTTCGTTTTTCGGCGCGAGCGGTTTCGGTTCGGGTTCGGCGCGGGGATGGACGGTTTCGGGGTTAGCGTCGTGGTCGTGCGCGTCGGTATTTCGGATTTGTAGTAGA				**GGTTGATGTAGTTGAGT**TGTGTTGTTGTTGTTGTTGTTGTTTTTTTGTGGAGTTTTTGGAGTTGTTGTTTTTTGTGTTGGTTTTGGTTTTGGTTTTTTTGGTTTTTTTTTGTGTAGTGTGGTTGATGGGGTTTTGGTGGGGGGGAAGGGGGGGTTGGGGTGTTGTGTGGAGTTTTTGGGTGTTTTGTTTTTTGGTGTGAGTGGTTTTGGTTTGGGTTTGGTGTGGGGATGGATGGTTTTGGGGTTAGTGTTGTGGTTGTGTGTGTTG**GTATTTTGGATTTGTAGTAGA**			
Melt Temp (°C)	92,5	Amplikon Length	289	Melt Temp(°C)	90,8-85,7	Amplikon Length	289

Table 3. Primer Set 3: primer sequences, amplicon lengths, and melting temperatures for methylated (M) and unmethylated (UnM) templates

Primer Set 3			
SHANK3-F3 primer	GTTTTCGGGATTTGAGTTTA	SHANK3-R3 primer	CCTAAAAACTATAATTAAAAACGC
LENGTH	20	LENGTH	24
MELT TEMP	56,5	MELT TEMP	54,9

Annealing Temp:	53,5			Annealing Temp:	53		
Amplikon 3-M				**Amplikon 3-UnM**			
GTTTTCGGGATTTGAGTTTACGAGTTCGTTTCGTTGTAGAAGTGTTTGCGTTTGGATTCGGTCGCGTTCGTGTGGGTCGTTAAGTAGCGCGTGTTTT**GCGTTTTTAATTATAGTTTTTAGG**				**GTTTTTGGGATTTGAGTTTA**TGAGTTTGTTTTGTTGTAGAAGTGTTTGTGTTTGGATTTGGTTGTGTTTGTGTGGGTTGTTAAGTAGTGTGTGTTTT**GTGTTTTTAATTATAGTTTTTAGG**			
Melt Temp (°C)	87	Amplikon Length	122	Melt Temp(°C)	79,2	Amplikon Length	122

2- Bisulphite Conversion of gDNAs

For bisulfite conversion, the EZ DNA Methylation™ Kit (Zymo Research) was used following the manufacturer's protocol. The Human Methylated & Non-methylated DNA Set (D5014, Zymo Research), consisting of paired control DNAs (methylated and unmethylated, 250 ng/µL), was included to monitor conversion efficiency and to serve as PCR controls. Prior to bisulfite treatment, control DNAs were diluted 1:10, and 4 µL of each was subjected to conversion. Converted DNA was eluted in 10 µL and subsequently diluted 1:5 prior to PCR/HRM analysis.

3- qPCR and HRM Analysis

All assays were carried out on a LightCycler® 480 System (Roche) and a CFX96 Real-Time PCR Detection System (Bio-Rad). PCR reactions were performed in a total volume of 20 µL, containing SOLIS BIODYNE Hot FirePol® EvaGreen® HRM Mix (5×), 400 nM of each primer, and 4 µL of bisulfite-converted DNA template. Post-conversion DNA was not quantified; instead, a fixed template volume (4 µL per 20 µL reaction) was used.

Annealing temperature optimization was performed using a gradient PCR (52–60 °C) with converted methylated and unmethylated control DNAs.

HRM analyses were performed using the LightCycler® 480 Software (Gene Scanning module, Roche) and CFX Maestro Software with the Precision Melt Analysis module (Bio-Rad). In all experiments, reactions were run in duplicate using bisulfite-converted control gDNAs (methylated and unmethylated) as templates. No-template controls (NTCs) were consistently included in parallel to monitor nonspecific amplification.

RESULT

Bisulfite conversion controls

Bisulfite conversion was successfully verified using the DAPK1 control assay included in the commercial kit (Zymo D5014). Amplification was obtained at the expected melting temperatures, confirming complete conversion of unmethylated cytosines and overall PCR competency. Both methylated and unmethylated human gDNAs provided by the manufacturer amplified as expected, validating the conversion and serving as positive and negative controls throughout the study. Representative amplification and melting curves for the methylated and unmethylated DAPK1 controls are shown in Figure 2.

Amplification and melt curve evaluation of SHANK3 primer sets

Among the three primer sets tested, Primer Sets 1 and 3 consistently produced amplification, yielding melt peaks at the expected temperatures (Figures 2–3). Primer Set 2, however, showed weak or inconsistent amplification and was therefore excluded from further analyses (Figure 4).

Gradient PCR optimization

Gradient PCR (52–60 °C) was carried out to determine optimal annealing conditions. For both Primer Sets 1 and 3, an annealing temperature of 54 °C yielded the most efficient and specific amplification, as evidenced by sharp melt peaks with minimal background signal (Figure 5).

Non-template controls and nonspecific amplification

In Primer Set 1, non-template controls (NTCs) showed late-cycle amplification. However, the derivative melting curves demonstrated that these products exhibited melting temperatures lower than the expected amplicon (Figure 6), and thus did not interfere with interpretation. In Primer Set 3, similar nonspecific amplification was observed, including in some template-containing reactions (Figure 7), but the products were again distinguished by their substantially lower melting temperatures compared to the target amplicon. In both cases, the presence of the correct product was still readily confirmed in template-containing wells.

Assay applicability

Primer Sets 1 and 3 enabled discrimination between methylated and unmethylated control DNAs (Figures 2–3, 7), supporting their use for SHANK3 methylation analysis by HRM. However, based on current data, the assay is most appropriate for qualitative "methylated vs. unmethylated" classification. Further validation, including determination of the limit of detection (LOD), limit of quantification (LOQ), and analytical sensitivity parameters, would be required to establish quantitative performance.

Discussion

In this study, a high-resolution melting (HRM) assay was developed and tested for the analysis of DNA methylation within a CpG island located upstream of exon 3 of the SHANK3 gene. By integrating in silico CpG island prediction, bisulfite conversion, and HRM-based analysis, we established a locus-specific workflow that enabled the discrimination of methylated and unmethylated templates.

The bisulfite conversion process was verified using the DAPK1 control assay and commercially available methylated and unmethylated DNAs. The successful amplification of these controls at expected melting temperatures confirmed the efficiency of conversion and the validity of subsequent HRM analysis. Among the three primer sets designed, Primer Sets 1 and 3 demonstrated consistent amplification and reliable discrimination between methylated and unmethylated templates, while Set 2 was less efficient. Gradient PCR optimization further established 54 °C as the optimal annealing temperature, ensuring reproducible performance.

Some nonspecific amplification events were observed in non-template controls (NTCs) and, to a lesser extent, in template-containing wells. However, these products displayed melting temperatures distinct from the expected amplicon, and thus did not interfere with interpretation. This observation underscores the importance of HRM curve analysis as a powerful tool for distinguishing true targets from nonspecific products.

The established assay is particularly suitable for qualitative "methylated versus unmethylated" classification. At this stage, the method cannot be considered quantitative, as validation parameters such as the limit of detection (LOD), limit of quantification (LOQ), and analytical sensitivity were not determined. Future work should address these parameters and evaluate assay performance across independent DNA samples to fully establish analytical robustness.

Despite these limitations, the present work provides an essential methodological foundation for SHANK3 methylation analysis. The primer sets and optimized HRM conditions reported here can serve as a basis for further investigations of SHANK3 epigenetic regulation in both research and diagnostic contexts.

Conclusion

This study describes the development of a locus-specific HRM assay for the analysis of DNA methylation in the SHANK3 gene. By combining in silico CpG island prediction, bisulfite conversion, and HRM optimization, we established primer sets and experimental conditions that enable clear discrimination between methylated and unmethylated templates. While the current assay is best suited for qualitative methylation assessment, further validation including LOD, LOQ, and analytical sensitivity studies will be required to extend its application to quantitative analyses. Overall, this work provides a methodological framework that may support future epigenetic investigations of SHANK3.

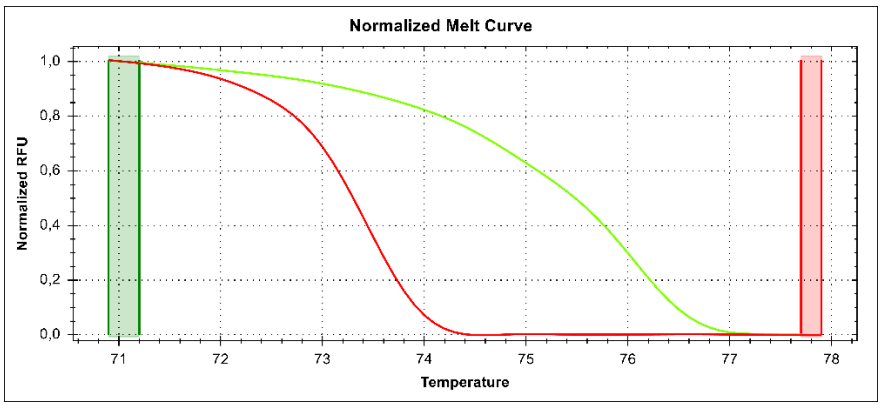

Figure 2. Normalized melt curves of BC unmethylated and methylated controls (Primer Set 1).

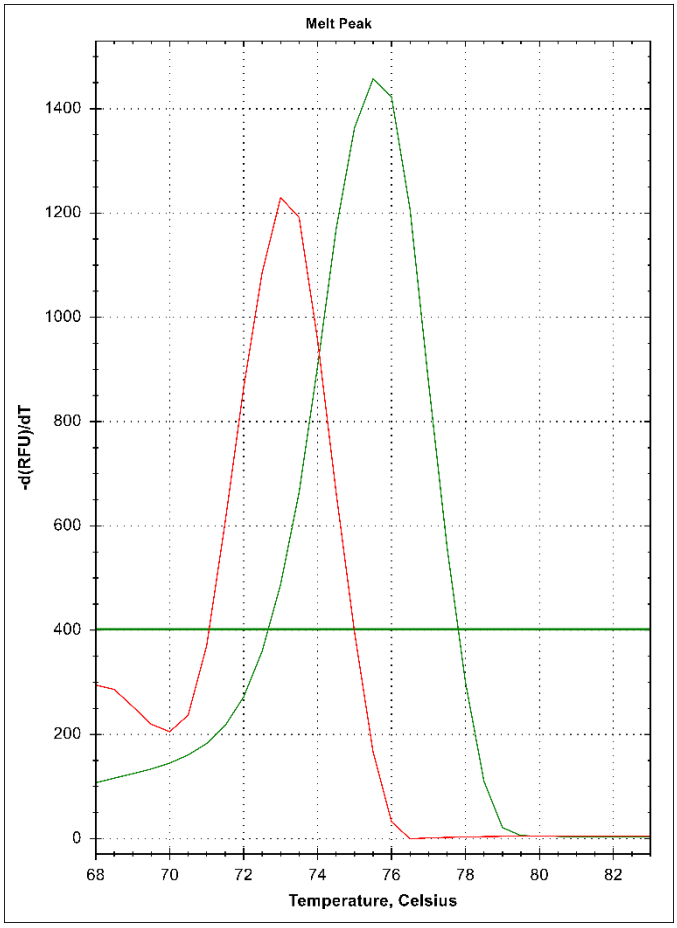

Figure 3. Melt peaks of BC unmethylated and methylated controls (Primer Set 1).

Tablo 1. Melting temperature values of BC Methylated and Unmethylated controls (Primer Set 1)

Target Set 1) (with Primer Set 1)	Melting Tempture
UnMeth Control	73.00
Meth Control	75.50

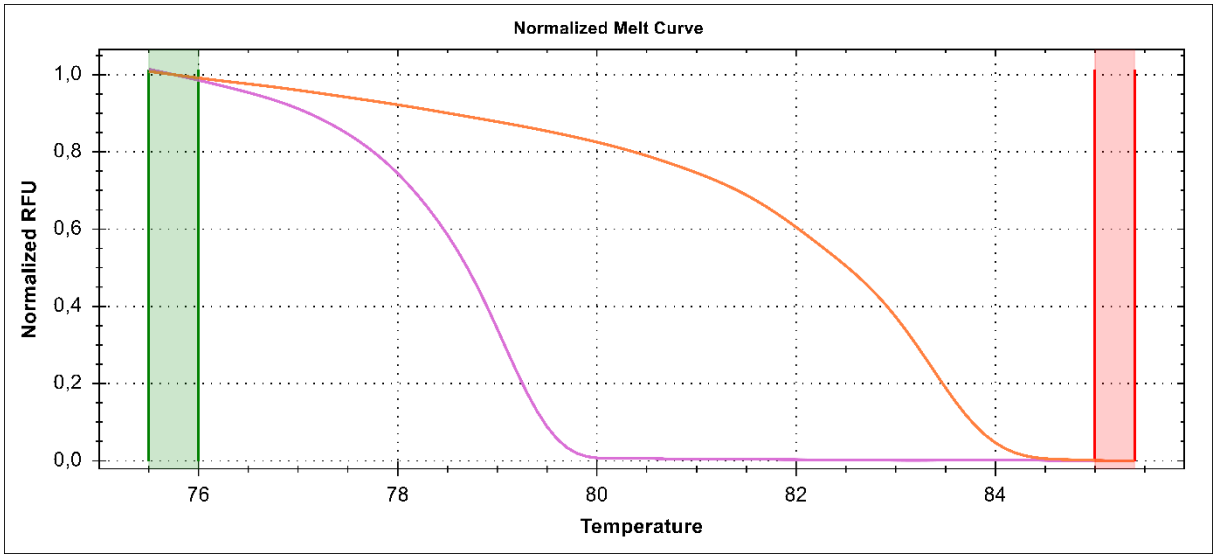

Figure 4. Normalized melt curves of BC unmethylated and methylated controls (Primer Set 2).

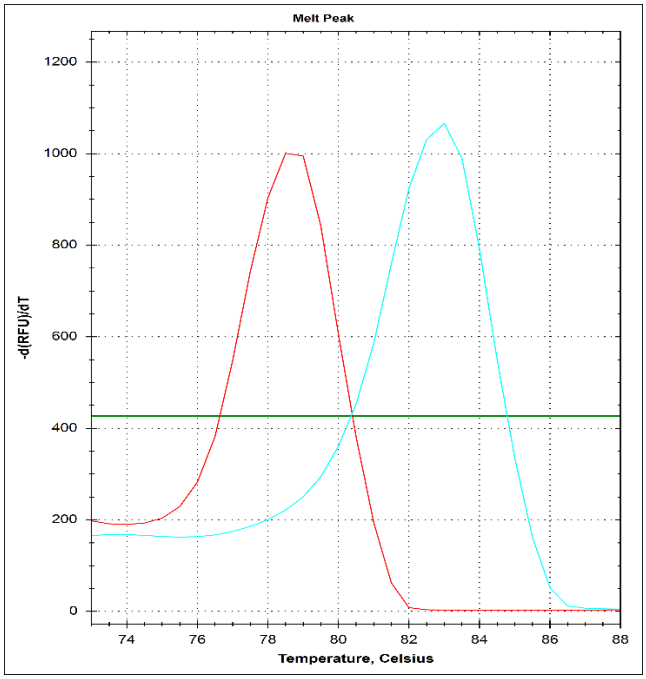

Figure 5. Melt peaks of BC unmethylated and methylated controls (Primer Set 2).

Table 1. Melting temperature values of BC Methylated and Unmethylated controls (Primer Set 2)

Target Set 2 (with Primer Set 2)	Melting Tempture
UnMeth Control	78.50
Meth Control	83,00

References (örnek, Vancouver tarzında)

1. Druml T, Cichna-Markl M. Detection of single CpG methylation events using quantitative PCR with methylation-sensitive high resolution melting. *Epigenetics*. 2014;9(6):760–771.
2. Wu X, Zhang Y. TET-mediated active DNA demethylation: mechanism, function and beyond. *Nat Rev Genet*. 2017;18(9):517–534.
3. Zhao J, Li M, Bradfield JP, et al. Promoter methylation as a biomarker in cancer detection and prognosis. *Clin Epigenetics*. 2022;14:125.
4. Shi D, Ma L, Zhao C, et al. Aberrant DNA methylation of cancer-related genes in human cancers. *Oncol Lett*. 2019;18(3):2901–2911.
5. Zhang W, Xu J, Wu J, et al. DNA methylation in promoter regions as biomarkers for cancer detection and therapy. *J Hematol Oncol*. 2015;8:34.
6. Mio C, Damante G. DNA methylation and cancer biomarkers. *Cancers (Basel)*. 2022;14(3):723.
7. Ma X, Cao X, Guo J. DNA methylation biomarkers for early detection of cancer. *Oncotarget*. 2016;7(9):11312–11325.
8. Dong C, Yin H, Yuan L, et al. Role of DNA methylation in cancer diagnosis and therapy. *Cancer Sci*. 2021;112(9):3532–3544.
9. Nguyen C, Liang G, Jones PA. DNA methylation changes associated with cancer. *J Natl Cancer Inst Monogr*. 2001;2001(27):55–66.
10. Yan PS, Chen CM, Shi H, et al. Dissecting complex epigenetic alterations in human breast cancers using CpG island microarrays. *Cancer Res*. 2003;63(12):3567–3575.
11. Tang X, Khuri FR, Lee JJ, et al. Hypermethylation of the death-associated protein kinase (DAPK) promoter in cancer. *Clin Cancer Res*. 2012;18(8):2284–2295.
12. Laurent L, Wong E, Li G, et al. Dynamic changes in the human methylome during differentiation. *Genome Res*. 2010;20(3):320–331.
13. Luo C, Hajkova P, Ecker JR. Dynamic DNA methylation: in the right place at the right time. *Science*. 2018;361(6409):1336–1340.
14. Barua S, Junaid MA. Genome-wide epigenetic analysis of autism. *Epigenomics*. 2014;6(3):343–355.
15. Grayson DR, Dunn EC. Epigenetic mechanisms in psychiatric disease. *Dialogues Clin Neurosci*. 2021;23(3):223–235.
16. Megagiannis P, et al. SHANK3 and synaptopathies: from genes to therapy. *Neurobiol Dis*. 2022;169:105730.

17. Cooke SF, et al. Shank3 deficiency: synaptic, circuit and behavioral insights. *Mol Psychiatry*. 2022;27:1811–1824.

18. Loth E, et al. The contribution of SHANK3 to autism: new insights from human and mouse models. *Mol Psychiatry*. 2017;22:1–12.

19. Wojdacz TK, Borgbo T, Hansen LL. Primer design versus PCR bias in methylation independent PCR amplifications. *Epigenetics*. 2009;4(4):231–236.

20. Park HC, Choi S, Lee J, et al. Enhanced sensitivity of CpG island search and primer design. *Forensic Sci Int Genet*. 2018;33:76–82.